mater.scichina.com link.springer.com

Published online 8 April 2022 | https://doi.org/10.1007/s40843-021-2003-5
Sci China Mater 2022, 65(7): 1971–1979

Nature-inspired nanothylakoids for multimodal cancer therapeutics

Hao Zhao[1,2], Yuduo Guo[1], Anran Yuan[1], Shengpeng Xia[1,2], Zhiqiang Gao[1,2], Yiming Huang[1*], Fengting Lv[1*], Libing Liu[1,2] and Shu Wang[1,2*]

ABSTRACT **Multimodal therapy has been recognized as a powerful platform for the precise treatment of cancer. However, the reported multimodal therapeutic systems often involve sophisticated components and tedious fabrication procedures. As such, developing nature-inspired and easily-obtainable theranostic agents for multimodal cancer therapy remains challenging. In this work, we propose nature-inspired nanothylakoids as a multimodal theranostic agent for cancer therapy both *in vitro* and *in vivo*. Nanothylakoids extracted from spinach leaves exhibit prominent photothermal and photodynamic inactivation on 4T1 and MCF-7 cancer cells due to their outstanding photothermal conversion/photosensitization capabilities. Additionally, the peroxidase-like catalytic activity of nanothylakoids is simultaneously verified, which facilitates the oxidation of H_2O_2 to the cytotoxic hydroxyl radical (·OH) and thus cause efficient cell apoptosis. Interestingly, a selective cytotoxicity of nanothylakoids on MCF-7 cancer cells is found due to their overexpression of H_2O_2. *In vitro* and *in vivo* results substantiate the prominent therapeutic outcome and excellent biosafety of nanothylakoids. Nanothylakoids with photothermal/photodynamic effects and peroxidase-like catalytic activity open a new avenue for the development of nature-inspired theranostic materials, holding great promise in multimodal cancer therapeutics.**

Keywords: nanothylakoids, multimodality, therapeutics

INTRODUCTION

Malignant cancers remain one of the most life-threatening diseases because of the tremendous difficulties in early diagnosis, efficient therapy, and poor prognosis [1–3]. Although chemotherapy is one of the most commonly used methods in clinics for cancer treatment, the therapeutic outcome is often limited due to the poor targeting capacities and severe side effects [4–6]. Meanwhile, the complicated tumor microenvironment makes patients readily susceptible to multidrug resistance (MDR), which further reduces the therapeutic outcome [7–10]. In the past decades, extensive advanced cancer therapeutic strategies have been developed for preclinical or clinical investigations, including phototherapy [11–15], radiotherapy [16,17], and immunotherapy [18–20]. Among them, photodynamic therapy (PDT) and photothermal therapy (PTT) lead to irreversible cell death by toxic reactive oxygen species (ROS) or localized heat post optical irradiation [21]. These two strategies have been regarded as the most attractive phototherapeutic approaches because of their high therapeutic efficiency, low side effects, and low possibility to cause MDR [22]. To enrich the library of high-quality phototherapeutic agents for disease treatments, a variety of functional materials have been successfully established in view of their prominent light-harvesting capacities in the visible or near infrared (NIR) region, including porphyrin and other small organic molecules [11,23], conjugated polymers [12,24], gold-based materials [25,26], carbon materials [27,28], and other nanomaterials [29,30]. Although these synthetic photoactive agents exhibit desirable performance in cancer phototherapeutics, the construction of multimodal therapeutic systems typically involves sophisticated components and tedious fabrication procedures [31]. Thus, it is still essential to pursue novel and easily available phototherapeutic nanoagents for tumor treatments, preferably with multimodal features, excellent biocompatibility, and less possibility to cause MDR.

Nature-inspired therapy systems, especially the plant- or microorganism-derived biomedical materials, have emerged as a class of promising candidates for cancer phototherapeutics. For instance, a biohybrid system composed of photosynthetic cyanobacterial cells and photosensitizer chlorine 6 was developed for oxygen-suppliable PDT [32], *Chlorella pyrenoidosa*-based light-triggered oxygen-affording engines were specifically proposed for repeated hypoxia-resistant PDT [33], and a plant-inspired photosynthetic abiotic/biotic nanoparticle system was also designed for normalizing the tumor microenvironment [34]. These efforts remarkably enriched the nature-inspired theranostic systems for cancer therapy. Nevertheless, the present studies primarily focused on the photosynthetic oxygenation to improve PDT efficiency. The direct utilization of plant- or microorganism-derived biomedical materials as the phototheranostic nanoplatform remains rarely explored. Moreover, motivated by the overexpressed H_2O_2 in the tumor microenvironment, the catalytical conversion of H_2O_2 into hydroxyl radical (·OH) has been proven to be a highly effective approach for the treatment of malignant cancers due to the high toxicity of ·OH [35–37]. Compared with the expensive natural enzymes and artificial nanozymes, the plant- or microorganism-derived multifunctional materials with built-in enzymatic activity can be obtained from widespread sources and/or *via* simple fabrication procedure, making them highly attractive in cancer therapy. Thus, the development of novel nature-derived materials with

[1] Beijing National Laboratory for Molecular Sciences, Key Laboratory of Organic Solids, Institute of Chemistry, Chinese Academy of Sciences, Beijing 100190, China
[2] College of Chemistry, University of Chinese Academy of Sciences, Beijing 100049, China
[*] Corresponding authors (emails: ymhuang@iccas.ac.cn (Huang Y); lvft@iccas.ac.cn (Lv F); wangshu@iccas.ac.cn (Wang S))

multimodal therapeutic functions will maximize cancer therapy and further broaden the category of bioinspired nanotheranostic tools.

Herein, we report plant leave-derived nanothylakoids with photothermal/photodynamic and peroxidase (POD)-like activities for enhanced cancer photo-therapeutics. As shown in Scheme 1, nanothylakoids are extracted from spinach leaves and exhibit multimodal therapeutic functions to cause cell death, that is, PDT- and PTT-capabilities and POD-like catalytic activity (converting H_2O_2 to ·OH). The multifunctional nanothylakoids show outstanding cancer therapeutic efficiency and excellent biosafety both *in vitro* and *in vivo*. Interestingly, a selective cytotoxicity of nanothylakoids to MCF-7 over 4T1 and a normal cell line, human pulmonary fibroblasts (HPF), is found, which can be attributed to the overexpressed H_2O_2 in the tumor microenvironment. This work provides a concept of using plant-derived photoactive nanomaterials for multimodal cancer therapeutics, holding great promise for future clinical uses.

EXPERIMENTAL SECTION

Photothermal property of nanothylakoids

Nanothylakoid solutions (60, 40, 20, 10, 5 μg mL^{-1}) were irradiated with laser (655 nm, 0.5 W cm^{-2}) for 5 min. The temperature-changing curve was recorded with a Ti400 thermal imaging camera. Water was applied as a control under the same experimental conditions.

Photodynamic property of nanothylakoids

The photodynamic property of nanothylakoids was confirmed by detecting the production of ROS. 2′,7′-Dichlorofluorescein (DCFH) was used as an ROS probe. Briefly, nanothylakoid solution (10 μg mL^{-1}) containing DCFH (40 μmol L^{-1}) was irradiated with a 655-nm laser or white light (10 mW cm^{-2}) for 7 min, and the fluorescence intensity at 525 nm was recorded with the excitation wavelength of 488 nm.

Peroxidase-like catalytic activity of nanothylakoids

The peroxidase activity of freshly isolated nanothylakoids was confirmed by detecting ·OH with the ultraviolet-visible (UV-vis) absorption of 3,3′,5,5′-tetramethylbenzidine (TMB). The absorption spectra of sodium acetate (NaAc) buffer (50 mmol L^{-1}, pH 4.7) containing nanothylakoids (20 μg mL^{-1}), H_2O_2 (50 mmol L^{-1}), and TMB (330 μmol L^{-1}) were measured for 10 min every 2 min. The NaAc buffer (50 mmol L^{-1}, pH 4.7) containing nanothylakoids/TMB, nanothylakoids/H_2O_2, and TMB/H_2O_2 was used as control under the same experimental conditions.

In vitro dark cytotoxicity of nanothylakoids

3-(4,5-Dimethylthiazol-2-yl)-2,5-diphenyltetrazolium bromide (MTT) assay was employed to evaluate the dark and photo-therapeutic toxicity of nanothylakoids. Briefly, for the dark toxicity of nanothylakoids, HPF, MCF-7, and 4T1 cells were seeded in 96-well plates at a density of 5 × 10^3 cells/well and cultured in the corresponding medium at 37°C for 12 h. Then,

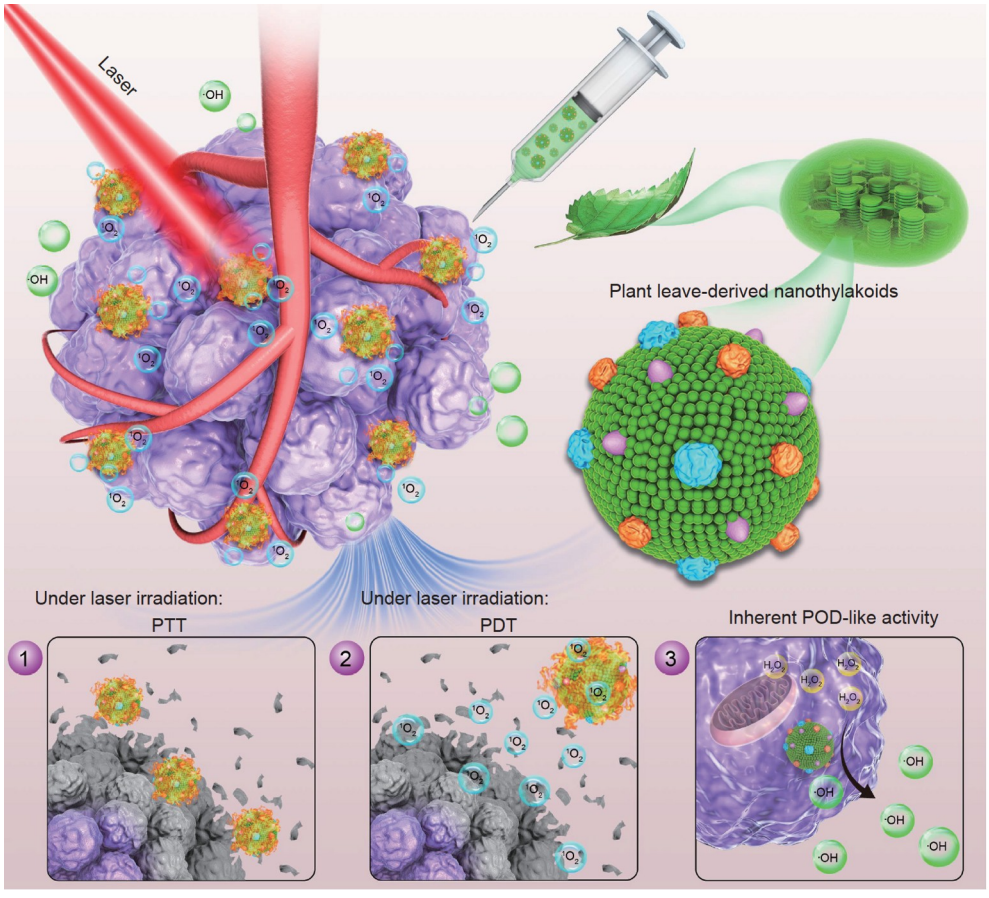

Scheme 1 Scheme of plant leave-inspired nanothylakoids for multimodal phototheranostics.

the medium containing nanothylakoids (0, 2.5, 5, 10, 20, 40, 80, and 100 μg mL^{-1}) was utilized to treat the cells at 37°C for 24 h. The medium was discarded and MTT (0.5 mg mL^{-1}, 100 μL well^{-1}) was added to the wells followed by incubation at 37°C for another 4 h. The supernatant was removed and dimethyl sulfoxide (DMSO, 100 μL per well) was added to dissolve the produced formazan. After shaking the plates for 3 min, all the absorbance of the wells was read with a microplate reader at 570 nm. The cell viability rate (VR) was calculated according to the following equation:

$$\mathrm{VR} = A / A_0 \times 100\%, \quad (1)$$

where A was the absorbance of the experimental group and A_0 was the absorbance of the control group, where control groups were carried out without nanothylakoids.

In vitro phototherapeutic cytotoxicity of nanothylakoids

MCF-7 and 4T1 were seeded in 96-well plates at a density of 5 × 10^3 cells/well and cultured in the corresponding medium at 37°C for 12 h. Then, the medium containing nanothylakoids (20 μg mL^{-1}) was utilized to treat the cells at 37°C for 6 h. The cells were irradiated with or without 655-nm laser (0.8 W cm^{-2}) for 5 min. After the irradiation, the cells were cultured for 24 h. Then the medium was discarded and MTT (0.5 mg mL^{-1}, 100 μL per well) was added to the wells followed by incubation at 37°C for another 4 h. The supernatant was removed and DMSO 100 μL well^{-1}) was added to dissolve the produced formazan. After shaking the plates for 3 min, all the absorbance of the wells was read with the microplate reader at 570 nm. The cell VR was calculated according to the above equation. For white light-triggered PDT of nanothylakoids to tumor cells, the procedure was identical except for the cells irradiated with or without white light (20 mW cm^{-2}) for 30 min.

Live/dead cell imaging

4T1 cells and MCF-7 cells were seeded in confocal dishes at a density of 2 × 10^5 cells/well and cultured at 37°C for 12 h. Then, cells were treated with 20 μg mL^{-1} nanothylakoids or phosphate buffer saline (PBS) at 37°C for 6 h. The cells were subjected to dark or irradiated with 655-nm laser (0.8 W cm^{-2}) for 5 min. After the irradiation, the cells were cultured for another 24 h. After removing the medium, the cells were incubated with the fresh medium containing calcein-AM/PI for 30 min at 37°C. The cells were washed with PBS three times after removing the culture medium. Confocal images were then acquired. For white light-triggered PDT, the procedure was identical except for the cells irradiated with or without white light (20 mW cm^{-2}) for 30 min.

Intracellular H_2O_2 imaging

HPF, 4T1, and MCF-7 cells were seeded in confocal dishes at a density of 8 × 10^4 cells/well and cultured in the corresponding medium at 37°C for 12 h. Then, the cells were treated with 6 μmol L^{-1} dihydroergotamine 123 at 37°C for 30 min, and washed with PBS three times after removing the culture medium followed by taking confocal images.

In vivo mouse tumor model

All animal experiments were performed under the Guide for the Care and Use of Laboratory Animals and were approved by the Institutional Animal Care and Use Committee in compliance with Chinese law for experimental animals. BALB/c nude mice (female, 4–6 weeks, 15–18 g) were commercially obtained from Vital River Laboratory Animal Technology Co., Ltd. (Beijing, China). The mouse tumor model was established by injecting 200 μL of 4T1 or MCF-7 cell suspension with a concentration of 5 × 10^6 cells mL^{-1} on the right hip of each nude mouse. *In vivo* animal experiments were performed when the tumor volume was above 60 mm^3. The length (A) and width (B) of the tumor were measured by a vernier caliper. The tumor volume was calculated according to the following equation:

$$V_{\mathrm{tumor}} = (A \times B^2) / 2. \quad (2)$$

In vivo photothermal conversion

Tumor-bearing nude mice were *in situ* injected with saline (200 μL) or nanothylakoid solution (200 μL, 300 μg mL^{-1}). At 1 h post-injection, the tumor sites were irradiated with laser (655 nm, 0.8 W cm^{-2}) for 10 min. During the irradiation process, temperature changes were recorded with the Ti400 thermal imaging camera.

In vivo phototherapy of nanothylakoids

Tumor-bearing nude mice were randomly divided into four groups (n = 5). The tumor-bearing nude mice were subjected to laser irradiation (655 nm, 0.8 W cm^{-2}) for 10 min post *in situ* injections of nanothylakoid solution (200 μL, 300 μg mL^{-1}). The nude mice with injection of saline (200 μL), the nude mice with laser irradiation post-injection of saline (200 μL), and the nude mice with injection of nanothylakoid solution (200 μL, 300 μg mL^{-1}) were used as control groups. The body weight and tumor volume of the nude mice in each group were monitored. At the end of the treatment, the nude mice were sacrificed, all tumors from the four groups were harvested for evaluating the antitumor efficiency, and the major organs (including heart, liver, spleen, kidneys, and lung) were collected for hematoxylin and eosin (H&E) staining.

RESULTS AND DISCUSSION

Nanothylakoids were isolated from spinach leaves with a simple and biocompatible "top-down" strategy [38]. The photophysical properties of nanothylakoids were characterized and the results are displayed in Fig. 1a. Due to the light-absorbing unites of chlorophyll inserted in the thylakoid membranes [39], nanothylakoids exhibited strong absorption in the visible region of 400–550 nm and NIR region of 640–700 nm, which guaranteed their prominent PDT and PTT capabilities. And a characteristic emission spectrum in the range of 650–800 nm is presented. Dynamic light scattering (DLS) and zeta potential data revealed the size of nanothylakoids dispersed in water was 80 ± 10 nm with a negative charge of −31 mV, and the size was well consistent with transmission electron microscopy (TEM) results (Fig. 1b, c). The POD-like catalytical activity of nanothylakoids, catalyzing H_2O_2 into highly cytotoxic ·OH, was evaluated by the oxidation of TMB upon addition of H_2O_2 (Fig. 1d). As shown in Fig. 1e and f, in the presence of H_2O_2, the absorbance at 680 nm of nanothylakoids/TMB solution increased in a time-dependent manner due to the gradual formation of the oxidated charge-transfer complex. For the control groups, the absorbance of nanothylakoids/TMB, nanothylakoids/H_2O_2, and TMB/H_2O_2 solutions remained rarely changed (Fig. 1f and Fig. S1). These results confirmed the POD-like catalytic activity of nanothyla-

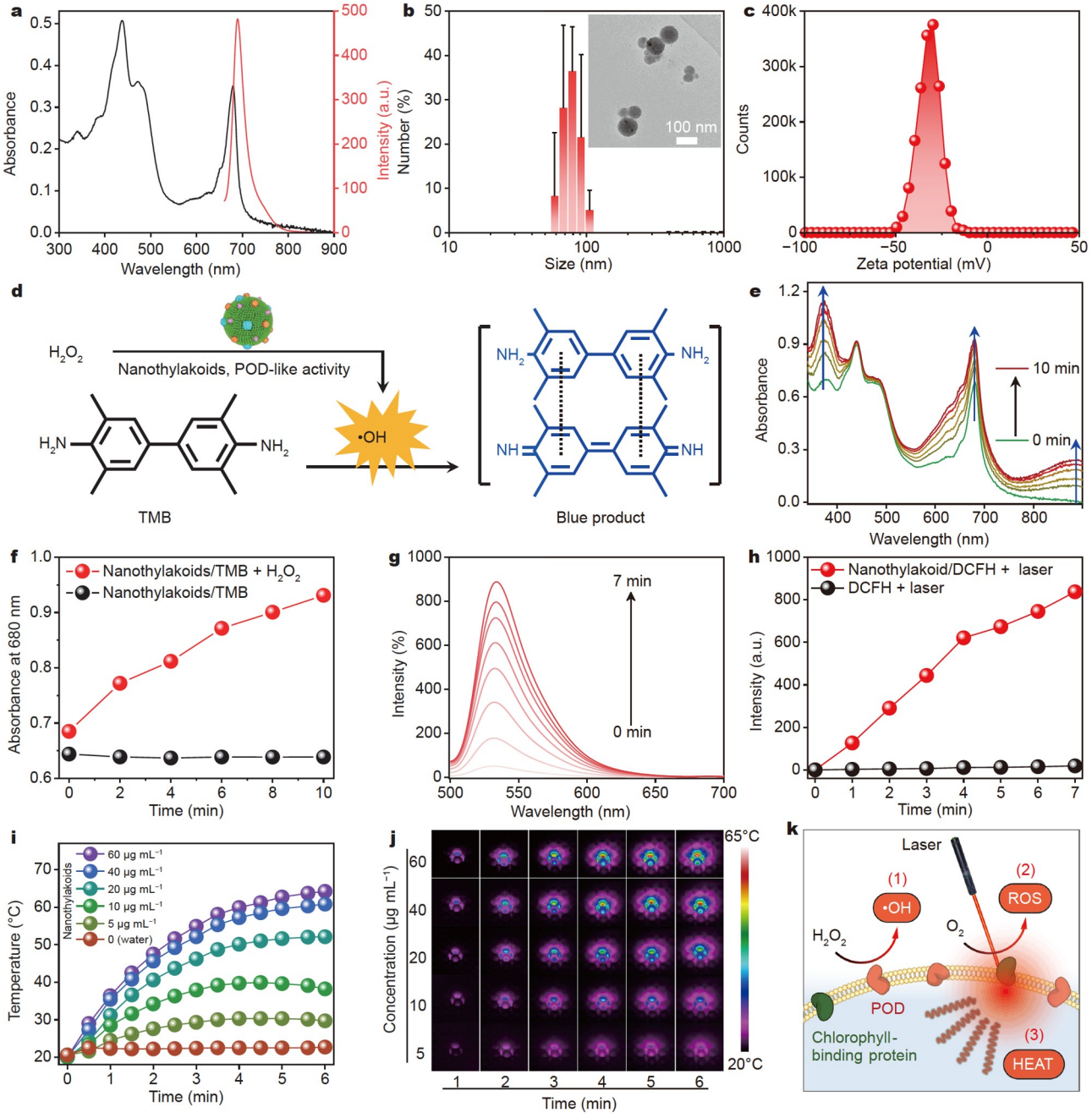

Figure 1 Material property characterizations and POD-like, photothermal/photodynamic activities of nanothylakoids. (a) Normalized absorption and emission spectra, (b) DLS (inset: TEM image of nanothylakoids), and (c) zeta potential of nanothylakoids in aqueous solution. (d) Illustration of the POD-like enzymatic reaction of nanothylakoids for converting TMB into blue products in the presence of H_2O_2. (e) Absorption spectra of nanothylakoids/TMB solution after addition of H_2O_2. (f) Time-dependent absorbance changes at 680 nm in (e). (g) Fluorescence spectra of DCFH solution with nanothylakoids upon laser irradiation (655 nm, 10 mW cm^{-2}). (h) Fluorescence rise rate of DCFH alone (control) and DCFH with nanothylakoid under laser irradiation (655 nm, 10 mW cm^{-2}). (i) Temperature-changing and (j) the corresponding infrared thermal images of various concentrations of nanothylakoids and water upon laser irradiation (655 nm, 0.5 W cm^{-2}). (k) Schematic illustration of the multimodal functions (POD-like activity, PDT, and PTT) of nanothylakoids.

koids. Natural enzymes and artificial nanozymes with POD-like properties have been reported [40,41]. Compared with the expensive natural enzymes with simple catalytical function, nanothylakoids were easily obtainable, and integrated with PDT/PTT multifunction, holding great promise in cancer therapy. In addition, artificial nanozymes made from carbon materials and metal complexes were limited in clinical use due to their potential toxicities, while the spinach leave-derived nanothylakoids exhibited enhanced biosafety. Given the strong light-harvest ability in the NIR region (650–800 nm), the photodynamic and photothermal conversion performance of nanothylakoids under 655-nm laser irradiation was investigated subsequently. The photodynamic property of nanothylakoids was demonstrated *via* detecting the generated ROS with a DCFH probe. As illustrated in Fig. 1g, nanothylakoids/DCFH solution showed an obvious fluorescence increment under laser irradiation (655 nm,

10 mW cm^{-2}). The NIR laser-triggered ROS generation of nanothylakoids was significantly higher than that of the control group of DCFH with 655-nm laser irradiation, reinforcing the excellent PDT effect of nanothylakoids (Fig. 1h). Besides, considering the absorption in the visible light region, the photodynamic property of nanothylakoids under white light irradiation was also assessed. As shown in Fig. S2, the fluorescence intensity of nanothylakoids/DCFH solution under white light irradiation (10 mW cm^{-2}) exhibited a time-dependent increment, which further verified the excellent PDT activity of nanothylakoids. Moreover, the photothermal conversion of nanothylakoids was investigated. As shown in Fig. 1i, various concentrations of nanothylakoids displayed significant photothermal conversion effect upon laser irradiation (655 nm, 0.5 W cm^{-2}), and the temperature of nanothylakoid solution indeed raised with the increment of concentrations and extension of irradiation time. With the concentration of 60 μg mL^{-1}, the temperature of the nanothylakoid solution increased to nearly 65°C after 5 min of irradiation. Even with a low concentration of 5 μg mL^{-1}, the photothermal conversion effect was still obvious. Under the identical conditions, there was negligible temperature increment for water, demonstrating the excellent photothermal conversion capability of nanothylakoids. The photothermal conversion efficiency (PCE) was calculated to be 30.8% [42]. The near-infrared thermal images (Fig. 1j) monitored the concentration-dependent and irradiation time-dependent photothermal temperature elevation process, which was well consistent with the results in Fig. 1i. These results validated that nanothylakoids could be a promising biomedical material for enzymic PDT/PTT multimodal cancer phototherapies.

The inherent cytotoxicity of nanothylakoids was evaluated before assessing their phototherapeutic effect against cancer cells. As shown in Fig. 2a, normal HPF cells exhibited a high cell survival rate treated with various concentrations of nanothylakoids, indicating the biocompatibility of nanothylakoids to normal cells. It was noted that the dark toxicity of nanothylakoids to cancer cell MCF-7 was significantly higher than that of HPF and 4T1, which motivated us to gain deep insight into the mechanism of the selectivity. Since the nanothylakoids with POD-like activity could catalyze the oxidation of H_2O_2 to highly toxic ·OH and lead to the cell apoptosis, the selective cytotoxicity could be attributed to the overexpression of H_2O_2. An intracellular H_2O_2 probe was utilized to directly visualize H_2O_2 expression inside of HPF, 4T1, and MCF-7 cells, respectively. As shown in Fig. 2b, confocal laser scanning microscopy (CLSM) images revealed that the fluorescence intensity distributed in MCF-7 cells was higher and more uniform than that of HPF and 4T1 cells, which was consistent with the results in the literature [43,44]. It could be concluded that the selective dark toxicity of nanothylakoids towards MCF-7 was attributed to the POD-like catalytic activity of nanothylakoids and the overexpression of H_2O_2 (Fig. 2c). The selective killing of tumor cells of nanothylakoids regulated by the tumor cell microenvironment held great promise in designing targeted multimodal tumor therapeutic agents.

Due to the multimodal therapeutic potentials demonstrated above, the PDT/PTT-integrated phototherapeutic effect of nanothylakoids on cancer cells was evaluated under 655-nm laser irradiation. After incubation for 6 h, nanothylakoids located inside or on the cell membrane of MCF-7 and 4T1 cells (Fig. S3), and the generated ROS and heat of nanothylakoids

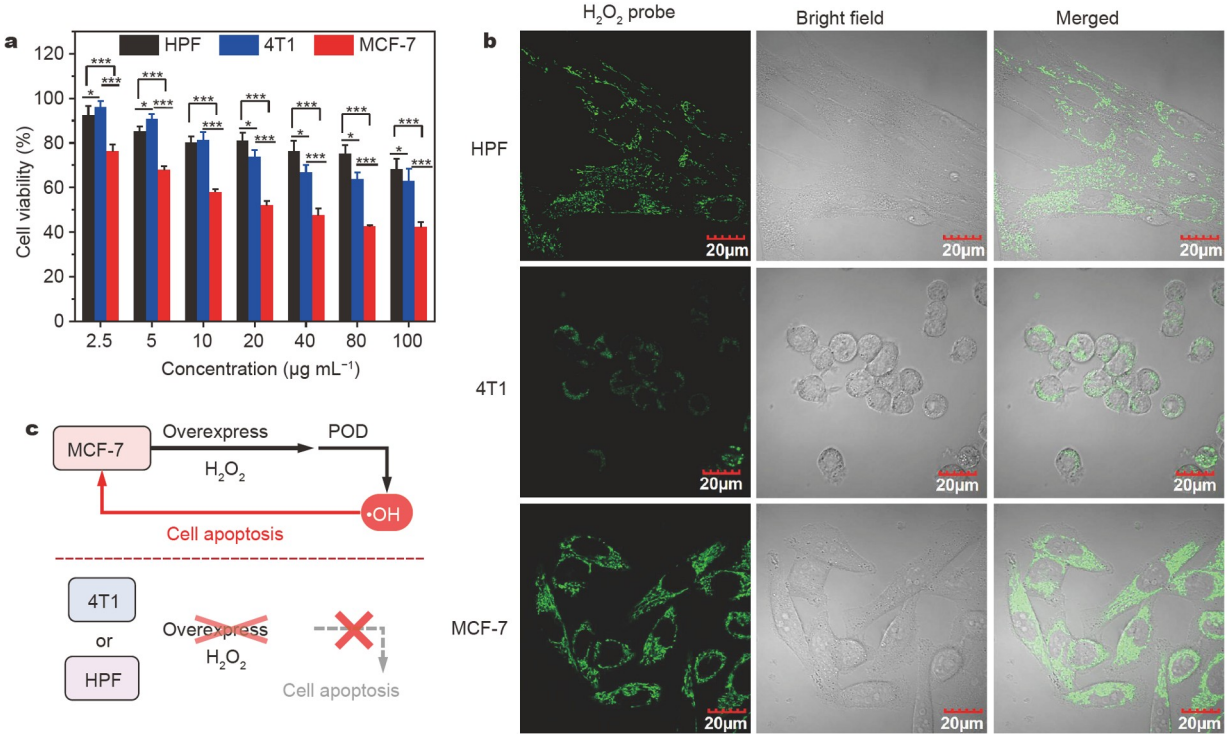

Figure 2 Cell toxicities of nanothylakoids towards HPF, 4T1, and MCF-7 cells without optical irradiation. (a) Cell viabilities of HPF, 4T1, and MCF-7 cells after treatment with various concentrations of nanothylakoids. n = 6, mean ± SD, * P < 0.05; ** P < 0.01; *** P < 0.001. (b) CLSM images of HPF, 4T1, and MCF-7 after treatment with intracellular H_2O_2 probe. (c) The proposed mechanism of the selective cell toxicity of nanothylakoids to MCF-7 cells in comparison with HPF and 4T1 cells.

upon laser irradiation are close enough to induce cell death. As shown in Fig. 3a and c, in the absence of nanothylakoids, 4T1 and MCF-7 cells exposed to 655-nm laser (0.8 W cm^{-2}, 5 min) irradiation kept high cell viabilities (almost 100%), suggesting the biosafety and noninvasiveness of laser as the optical therapeutic tool. However, in the presence of nanothylakoids, the cell survival rates of 4T1 and MCF-7 significantly decreased with increasing concentration of nanothylakoids after laser irradiation, exhibiting a concentration-dependent manner. Almost 80% 4T1 and more than 80% MCF-7 cancer cells were killed when treated by 20 μg mL^{-1} nanothylakoids, and the killing efficiency to MCF-7 was higher than that of 4T1 due to the dark toxicity of nanothylakoids towards MCF-7. Live/dead cell CLSM images were further utilized to visualize the phototherapeutic effect of nanothylakoids. As shown in Fig. 3b, for 4T1 cancer cells, green signal represented living cells for laser and nanothylakoids group, indicating the high cell survival rate. While for the phototherapeutic group, red signal in CLSM images represented dead cells, demonstrating that 4T1 cancer cells were completely killed after laser irradiation. The same results were also observed for MCF-7 cancer cells, where nanothylakoids group exhibited strong red signals of dead cells with laser irradiation (Fig. 3d). In addition, nanothylakoids also exhibited a good PDT cancer cell killing effect to 4T1 and MCF-7 cells upon white light irradiation (Fig. S4). These results confirmed that nanothylakoids could be utilized as promising PDT and PTT agents for cancer cell therapy *in vitro*.

As NIR laser has better tissue penetration capacity than white light, the *in vivo* nanothylakoid-based phototherapeutics triggered by 655-nm laser was studied on the tumor-bearing nude mouse model. 4T1 tumor-bearing nude mice were divided into four groups, nanothylakoids with laser irradiation, saline with laser irradiation, nanothylakoids, and saline. For nanothylakoids with laser irradiation group, the nude mice were injected with the nanothylakoid solution (200 μL, 300 μg mL^{-1}) followed by irradiation with 655-nm laser (0.8 W cm^{-2}) for 10 min. Thermal infrared images were collected during the phototherapeutic process and the temperature variations in the irradiated-tumor area were also monitored. As shown in Fig. 4a and b, for nanothylakoids with laser irradiation group, the localized temperature of the tumor sites increased to nearly 90°C after 10 min of laser irradiation, which was higher than that of the other three groups. These results confirmed the robust *in vivo* photothermal conversion effect of nanothylakoids. It is worth

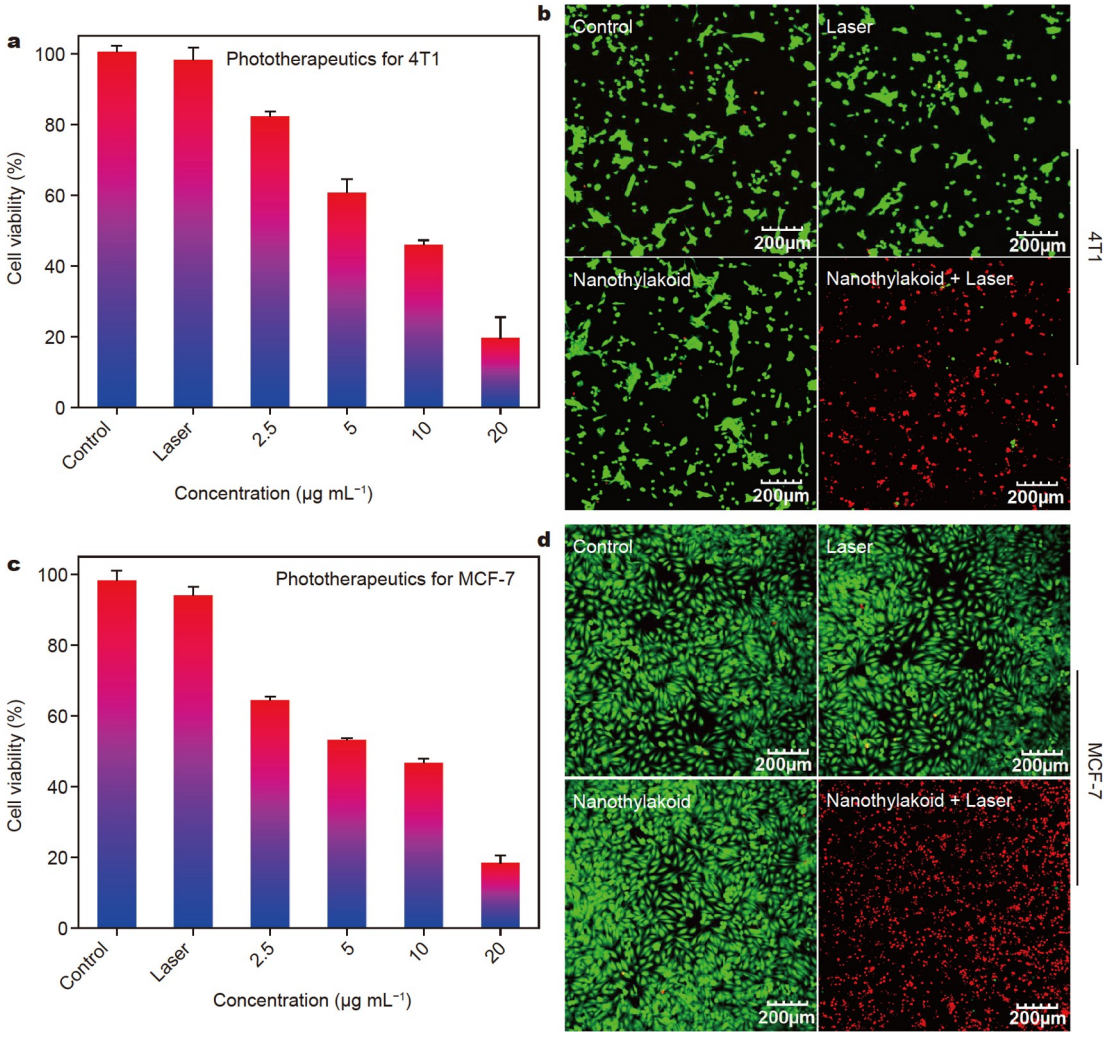

Figure 3 Multimodal phototherapeutic effect of nanothylakoids to 4T1 and MCF-7 cancer cells *in vitro*. Cell survival rates of (a) 4T1 and (c) MCF-7 cells after treatment with nanothylakoids upon laser irradiation (655 nm, 0.8 W cm^{-2}) for 5 min. Live/dead CLSM images of (b) 4T1 and (d) MCF-7 cells with various treatments (live: green, dead: red).

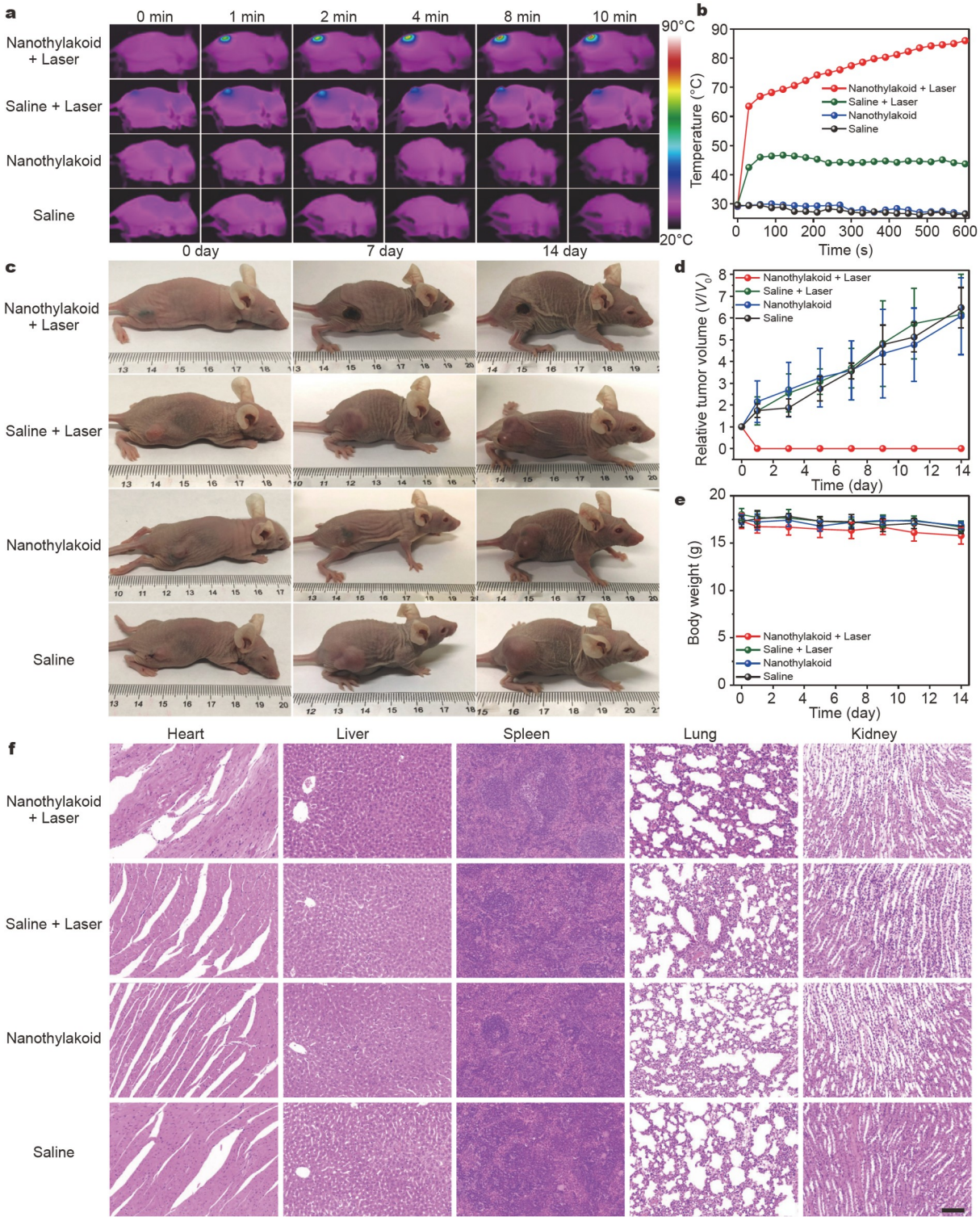

Figure 4 Multimodal phototherapeutic effect of nanothylakoids on 4T1 tumor-bearing nude mice *in vivo*. (a) Infrared thermal images and (b) temperature-changing curve of 4T1 tumor-bearing nude mice with or without nanothylakoid-treatment upon laser irradiation (655 nm, 0.8 W cm^{-2}) for 10 min. (c) Representative digital images of 4T1 tumor-bearing nude mice during the treatment process. (d) Relative tumor volume and (e) body weight changes of 4T1 tumor-bearing nude mice in the four treatment groups for 14 days. (f) H&E staining of the major organs dissected from the mice at day-14 after various treatments. Scale bar: 100 μm.

noting that the temperature increments only occurred in the irradiated tumor area, indicating the good spatiotemporal selectivity and promising potential of the nanothylakoid-based phototherapeutics. The tumor volume and body weight of the 4T1 tumor-bearing nude mice were monitored in the following 14 days. As shown in Fig. 4c and d, for the nanothylakoids with laser irradiation group, the tumor was ablated entirely and no relapse was found within 14 days. For the other three groups, the

tumors were growing up along with time without any inhibition. The body weights of all nude mice in the four groups changed negligibly, indicating the minimal toxicity of nanothylakoids to mice and good biosafety of the therapeutic conditions *in vivo* (Fig. 4e). After treatments, all the mice were euthanized for histological analysis of the main organs. As shown in Fig. 4f, H&E staining results displayed negligible systemic damage to the main organs including heart, liver, spleen, lung, and kidney in all groups after different treatments. These results highlight the prominent therapeutics efficiency, good biocompatibility, and biosafety of nanothylakoids as multimodal phototherapeutic nanoplatforms for cancer treatment in living animals. MCF-7 tumor-bearing nude mouse model was also established for *in vivo* phototherapeutic studies. As shown in Fig. S5a and b, for the nanothylakoids with laser irradiation group, the temperature of the tumor sites selectively increased to nearly 90°C, which was significantly higher than that of the other three groups, and the tumors were completely ablated without relapse within 12 days during the treatment process (Fig. S5c, d). It should be noted that compared with the saline group, a weaker tumor inhibition effect was observed similar to the *in vitro* data for the nanothylakoids group, which may be due to the complicated microenvironment of solid tumors (Fig. S5d). The negligible change of mouse body weight and less damage to the main organs of mice also verified the excellent biocompatibility and noninvasiveness of the nanothylakoid-based treatment nanoplatform (Fig. S5e, f).

The plant leave-derived nanothylakoids with multimodal therapeutic functions including PDT, PTT, and POD-like catalytic activity exhibited high therapeutic efficiency and desired biosafety. Different from the reported photosynthetic oxygenation to improve tumor PDT effect so far [32–34], we directly explored the plant-derived nanothylakoids as optically active and catalytic therapeutic agents to enhance cancer treatment efficacy, which provided more possibilities of natural materials for tumor remedy. Besides, the widespread sources and simplified "top-down" fabrication strategy of nanothylakoids significantly avoid the high-cost as well as tedious preparation and purification procedures of natural enzymes together with artificially synthetic materials. Improving the photo energy conversion and catalytical performances, the nanothylakoid-based theranostic agent will maximize cancer therapy and further broaden the category of bioinspired nanotheranostic tools.

CONCLUSIONS

In summary, we reported plant leave-derived nanothylakoids with POD-like and photothermal/photodynamic activities for multimodal cancer phototherapeutics with high therapy efficiency and outstanding biosafety both *in vitro* and *in vivo*. Importantly, a selective cytotoxicity of nanothylakoids on MCF-7 cancer cells was found due to their overexpression of H_2O_2, which facilitated the oxidation of H_2O_2 to the cytotoxic ROS and thus caused efficient cell apoptosis. This work provides a concept of plant-derived nanomaterials for multimodal cancer therapeutics based on enzymatic nanothylakoids, holding great promise for future clinical uses.

Received 11 December 2021; accepted 21 February 2022; published online 8 April 2022

1 Siegel RL, Miller KD, Jemal A. Cancer statistics, 2016. CA-Cancer J Clin, 2016, 66: 7–30
2 Yang G, Xu L, Chao Y, *et al.* Hollow MnO_2 as a tumor-microenvironment-responsive biodegradable nano-platform for combination therapy favoring antitumor immune responses. Nat Commun, 2017, 8: 902
3 Li N, Sun Q, Yu Z, *et al.* Nuclear-targeted photothermal therapy prevents cancer recurrence with near-infrared triggered copper sulfide nanoparticles. ACS Nano, 2018, 12: 5197–5206
4 Zha Z, Wang J, Qu E, *et al.* Polypyrrole hollow microspheres as echogenic photothermal agent for ultrasound imaging guided tumor ablation. Sci Rep, 2013, 3: 2360
5 Cheng L, Liu J, Gu X, *et al.* PEGylated WS_2 nanosheets as a multifunctional theranostic agent for *in vivo* dual-modal CT/photoacoustic imaging guided photothermal therapy. Adv Mater, 2014, 26: 1886–1893
6 Li S, Deng Q, Li X, *et al.* Bis-diketopyrrolopyrrole conjugated polymer nanoparticles as photothermic nanoagonist for specific and synergistic glioblastoma therapy. Biomaterials, 2019, 216: 119252
7 Hanahan D, Weinberg RA. Hallmarks of cancer: The next generation. Cell, 2011, 144: 646–674
8 Dean M, Fojo T, Bates S. Tumour stem cells and drug resistance. Nat Rev Cancer, 2005, 5: 275–284
9 Wang H, Feng Z, Qin Y, *et al.* Nucleopeptide assemblies selectively sequester ATP in cancer cells to increase the efficacy of doxorubicin. Angew Chem Int Ed, 2018, 57: 4931–4935
10 Zhou L, Lv F, Liu L, *et al. In situ*-induced multivalent anticancer drug clusters in cancer cells for enhancing drug efficacy. CCS Chem, 2019, 1: 97–105
11 Yang B, Chen Y, Shi J. Reactive oxygen species (ROS)-based nanomedicine. Chem Rev, 2019, 119: 4881–4985
12 Zhu C, Liu L, Yang Q, *et al.* Water-soluble conjugated polymers for imaging, diagnosis, and therapy. Chem Rev, 2012, 112: 4687–4735
13 Zhao H, Xu J, Yuan H, *et al.* 3D printing of artificial skin patches with bioactive and optically active polymer materials for anti-infection and augmenting wound repair. Mater Horiz, 2022, 9: 342–349
14 Cheng L, Wang C, Feng L, *et al.* Functional nanomaterials for phototherapies of cancer. Chem Rev, 2014, 114: 10869–10939
15 Elsabahy M, Heo GS, Lim SM, *et al.* Polymeric nanostructures for imaging and therapy. Chem Rev, 2015, 115: 10967–11011
16 Cutler CS, Hennkens HM, Sisay N, *et al.* Radiometals for combined imaging and therapy. Chem Rev, 2013, 113: 858–883
17 Goswami N, Luo Z, Yuan X, *et al.* Engineering gold-based radiosensitizers for cancer radiotherapy. Mater Horiz, 2017, 4: 817–831
18 Chen Q, Chen M, Liu Z. Local biomaterials-assisted cancer immunotherapy to trigger systemic antitumor responses. Chem Soc Rev, 2019, 48: 5506–5526
19 Irvine DJ, Hanson MC, Rakhra K, *et al.* Synthetic nanoparticles for vaccines and immunotherapy. Chem Rev, 2015, 115: 11109–11146
20 Han X, Shen S, Fan Q, *et al.* Red blood cell-derived nanoerythrosome for antigen delivery with enhanced cancer immunotherapy. Sci Adv, 2019, 5: eaaw6870
21 Guo Z, Zhou X, Hou C, *et al.* A chloroplast-inspired nanoplatform for targeting cancer and synergistic photodynamic/photothermal therapy. Biomater Sci, 2019, 7: 3886–3897
22 Zhou S, Yang C, Guo L, *et al.* Water-soluble conjugated polymer with near-infrared absorption for synergistic tumor therapy using photothermal and photodynamic activity. Chem Commun, 2019, 55: 8615–8618
23 Singh S, Aggarwal A, Bhupathiraju NVSDK, *et al.* Glycosylated porphyrins, phthalocyanines, and other porphyrinoids for diagnostics and therapeutics. Chem Rev, 2015, 115: 10261–10306
24 Li J, Pu K. Development of organic semiconducting materials for deep-tissue optical imaging, phototherapy and photoactivation. Chem Soc Rev, 2019, 48: 38–71
25 Huang P, Rong P, Lin J, *et al.* Triphase interface synthesis of plasmonic gold bellflowers as near-infrared light mediated acoustic and thermal theranostics. J Am Chem Soc, 2014, 136: 8307–8313
26 Skrabalak SE, Chen J, Au L, *et al.* Gold nanocages for biomedical applications. Adv Mater, 2007, 19: 3177–3184
27 Li S, Chen Y, Liu H, *et al.* Graphdiyne materials as nanotransducer for *in vivo* photoacoustic imaging and photothermal therapy of tumor.

Chem Mater, 2017, 29: 6087–6094
28 Wang X, Wang C, Cheng L, *et al.* Noble metal coated single-walled carbon nanotubes for applications in surface enhanced Raman scattering imaging and photothermal therapy. J Am Chem Soc, 2012, 134: 7414–7422
29 Wang X, Lv F, Li T, *et al.* Electrospun micropatterned nanocomposites incorporated with Cu_2S nanoflowers for skin tumor therapy and wound healing. ACS Nano, 2017, 11: 11337–11349
30 Zhao H, Xu X, Zhou L, *et al.* Water-soluble nanoparticles with twisted double [7]carbohelicene for lysosome-targeted cancer photodynamic therapy. Small, 2022, 18: 2105365
31 Ouyang J, Wang L, Chen W, *et al.* Biomimetic nanothylakoids for efficient imaging-guided photodynamic therapy for cancer. Chem Commun, 2018, 54: 3468–3471
32 Huo M, Wang L, Zhang L, *et al.* Photosynthetic tumor oxygenation by photosensitizer-containing cyanobacteria for enhanced photodynamic therapy. Angew Chem Int Ed, 2020, 59: 1906–1913
33 Zhou TJ, Xing L, Fan YT, *et al.* Light triggered oxygen-affording engines for repeated hypoxia-resistant photodynamic therapy. J Control Release, 2019, 307: 44–54
34 Zheng D, Li B, Xu L, *et al.* Normalizing tumor microenvironment based on photosynthetic abiotic/biotic nanoparticles. ACS Nano, 2018, 12: 6218–6227
35 Xu Z, Qiu Z, Liu Q, *et al.* Converting organosulfur compounds to inorganic polysulfides against resistant bacterial infections. Nat Commun, 2018, 9: 3713
36 Hu WC, Younis MR, Zhou Y, *et al. In situ* fabrication of ultrasmall gold nanoparticles/2D MOFs hybrid as nanozyme for antibacterial therapy. Small, 2020, 16: 2000553
37 Sun J, Du K, Diao J, *et al.* GSH and H_2O_2Co-activatable mitochondria-targeted photodynamic therapy under normoxia and hypoxia. Angew Chem Int Ed, 2020, 59: 12122–12128
38 Zhou X, Zhou L, Zhang P, *et al.* Conducting polymers-thylakoid hybrid materials for water oxidation and photoelectric conversion. Adv Electron Mater, 2019, 5: 1800789
39 Chu M, Li H, Wu Q, *et al.* Pluronic-encapsulated natural chlorophyll nanocomposites for *in vivo* cancer imaging and photothermal/photodynamic therapies. Biomaterials, 2014, 35: 8357–8373
40 Song Y, Qu K, Zhao C, *et al.* Graphene oxide: Intrinsic peroxidase catalytic activity and its application to glucose detection. Adv Mater, 2010, 22: 2206–2210
41 Huang Y, Ren J, Qu X. Nanozymes: Classification, catalytic mechanisms, activity regulation, and applications. Chem Rev, 2019, 119: 4357–4412
42 Zhao H, Huang Y, Lv F, *et al.* Biomimetic 4D-printed breathing hydrogel actuators by nanothylakoid and thermoresponsive polymer networks. Adv Funct Mater, 2021, 31: 2105544
43 Zhou L, Lv F, Liu L, *et al.* Cross-linking of thiolated paclitaxel-oligo(*p*-phenylene vinylene) conjugates aggregates inside tumor cells leads to "chemical locks" that increase drug efficacy. Adv Mater, 2018, 30: 1704888
44 Han Y, Ouyang J, Li Y, *et al.* Engineering H_2O_2 self-supplying nanotheranostic platform for targeted and imaging-guided chemodynamic therapy. ACS Appl Mater Interfaces, 2020, 12: 288–297

Acknowledgements The work was supported by the National Natural Science Foundation of China (22021002, 22020102005, and 22022705) and the Strategic Priority Research Program of the Chinese Academy of Sciences (XDA16020804).

Author contributions Huang Y, Lv F, and Wang S designed the research. Zhao H isolated the nanothylakoids and performed the experiments with Guo Y and Yuan A. Zhao H wrote the paper with support from Xia S, Gao Z, and Liu L. All authors contributed to the general discussion.

Conflict of interest The authors declare that they have no conflict of interest.

Supplementary information Experimental details and supporting data are available in the online version of the paper.

Hao Zhao received his PhD degree from the Institute of Chemistry, Chinese Academy of Sciences (ICCAS). His current research interest mainly focuses on conjugated polymer-nature-inspired bioactive materials for biomedical applications.

Yiming Huang obtained his BSc degree in chemistry from Nanjing University in 2009. He then joined the group of Prof. Dominic V. McGrath at University of Arizona. After completing his PhD in 2015, he worked as a postdoc research associate with Prof. Eilaf Egap at Emory University and Rice University. He joined the ICCAS in 2018. His research focuses on functional polymers for biomedical applications.

Fengting Lv received her BSc, MSc, and PhD degrees from Shaanxi Normal University in 2002, 2005, and 2008, respectively. She spent one year at Michigan State University as a joint PhD student. In 2009, she moved to the Institute of Chemistry, Chinese Academy of Sciences as a postdoctoral fellow in Prof. Wang's group, and became a professor in 2021. Her current research interest focuses on the design of water-soluble conjugated polymers for bioassembly and bioelectronics applications.

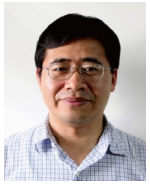

Shu Wang obtained his BSc degree from Hebei University in 1994, and then PhD degree at Peking University in 1999. He worked as a postdoctoral researcher at the ICCAS from 1999 to 2001, and at the University of California, Santa Barbara from 2001 to 2004. In 2004, he became a full professor at the ICCAS. His current research interests include the design and synthesis of novel conjugated polymers for disease therapeutic, biocatalysis, and organic bioelectronics.

天然来源的纳米类囊体应用于肿瘤的多模式治疗

赵浩[1,2], 郭玉铎[1], 袁安然[1], 夏晟鹏[1,2], 高志强[1,2], 黄一鸣[1*], 吕凤婷[1*], 刘礼兵[1,2], 王树[1,2*]

摘要 多模式联合治疗已成为抗肿瘤的有效手段, 但目前已报道的多模式肿瘤治疗试剂通常需要复杂的功能组分和繁琐的合成过程. 因此, 开发一种简单制备的天然来源多模式肿瘤治疗试剂仍然是一个挑战. 本文从菠菜叶片中提取出了一种天然来源的、具有类酶性质的纳米类囊体用于肿瘤的多模式治疗. 结果表明, 纳米类囊体具有良好的光热转换和光敏化性质, 可以有效杀伤4T1和MCF-7肿瘤细胞. 同时, 该材料还具有类过氧化物酶的性质, 可以氧化分解过氧化氢产生羟基自由基从而诱导肿瘤细胞凋亡. 因MCF-7肿瘤细胞内过量表达过氧化氢, 该材料可实现对MCF-7肿瘤细胞的选择性杀伤. 该纳米类囊体在细胞水平和活体小动物水平对肿瘤具有显著的治疗效果, 且表现出良好的生物安全性. 研究表明, 该纳米类囊体具有光热转换、光敏化、类过氧化物酶的性质, 是一类很有应用前景的多模式肿瘤治疗试剂.

